J. Membrane Biol. 171, 151–169 (1999)

The Journal of
Membrane
Biology

F-actin at Newly Invaginated Membrane in Neurons: Implications for Surface Area Regulation

T.L. Herring,[1] C.S. Cohan,[2] E.A. Welnhofer,[2] L.R. Mills,[3] C.E. Morris[4]

[1]Departments of Biology and Medicine, University of Ottawa, Ottawa, Ontario, Canada, K1Y4E9
[2]Department of Anatomy and Cell Biology, SUNY Buffalo, NY, 14214, USA
[3]Playfair Neuroscience Unit, The Toronto Hospital Research Institute, Toronto, Canada, M5T 2S8
[4]Neurosciences, Loeb Health Research Institute, Ottawa Hospital, Ottawa, Canada, K1Y 4E9

Received: 25 March 1999/Revised: 15 June 1999

Abstract. Neuronal shape and volume changes require accompanying cell surface adjustments. In response to osmotic perturbations, neurons show evidence of surface area regulation; shrinking neurons invaginate membrane at the substratum, pinch off vacuoles, and lower their membrane capacitance. F-actin is implicated in reprocessing newly invaginated membrane because cytochalasin causes the transient shrinking-induced invaginations, vacuole-like dilations (VLDs), to persist indefinitely instead of undergoing recovery. To help determine if cortical F-actin indeed contributes to cell surface area regulation, we test, here, the following hypothesis: invaginating VLD membrane rapidly establishes an association with F-actin and this association contributes to VLD recovery. Cultured molluscan (*Lymnaea*) neurons, whose large size facilitates three-dimensional imaging, were used. In fixed neurons, fluorescent F-actin stains were imaged. In live neurons, VLD membrane was monitored by brightfield microscopies and actin was monitored via a fluorescent tag. VLD formation (unlike VLD recovery) is cytochalasin insensitive and consistent with this, VLDs formed readily in cytochalasin-treated neurons but showed no association with F-actin. Normally, however (i.e., no cytochalasin), VLDs were foci for rapid reorganization of F-actin. At earliest detection (1–2 min), nascent VLDs were entirely coated with F-actin and by 5 min, VLD mouths (i.e., at the substratum) had become annuli of F-actin-rich motile leading edge. Time lapse images from live neurons showed these rings to be motile filopodia and lamellipodia. The retrieval of VLD membrane (vacuolization) occurred via actin-associated constriction of VLD mouths. The interplay of surface membrane and cortical cytoskeleton in osmotically perturbed neurons suggests that cell surface area and volume adjustments are coordinated in part via mechanosensitive F-actin dynamics.

Key words: Actin — Membrane cytoskeleton — Adhesion — Mechanoprotection — Membrane retrieval — Regulatory volume decrease — Molluscan neuron

Introduction

During development, neurons continually change their morphology. The cytoskeleton, via adhesion zones, monitors and responds to mechanical stresses (e.g., Ingber, 1997) but it is unclear how the surface membrane accommodates. By what means are changes in plasma membrane surface area coordinated with the changes in cell volume and shape? Observations during osmomechanically elicited volume and surface area changes in neurons suggest that membrane tension may provide feedback for surface area adjustments (Morris et al., 1997; Herring et al., 1998). More specifically, abruptly shrinking neurons behave as if plasma membrane area decreases to accommodate the reduced volume: (i) neuronal capacitance decreases at ~1 μF per apparent cm^2 decrease in surface area (Wan, Harris & Morris, 1995), (ii) tether force measurements indicate that membrane tension falls (Dai et al., 1998), perhaps facilitating the reinternalization of slack excess membrane (Morris et al., 1997), (iii) at the substratum where neurons are adherent, they invaginate plasma membrane in the form of vacuole-like dilations (VLDs) (Reuzeau et al., 1995; Mills & Morris, 1998; *see* Fig. 1*a*). VLDs appear to be exaggerated retrieval structures associated with surface area regulation. When shrinkage is initiated, they grow within minutes from submicroscopic invaginations to

Correspondence to: C.E. Morris

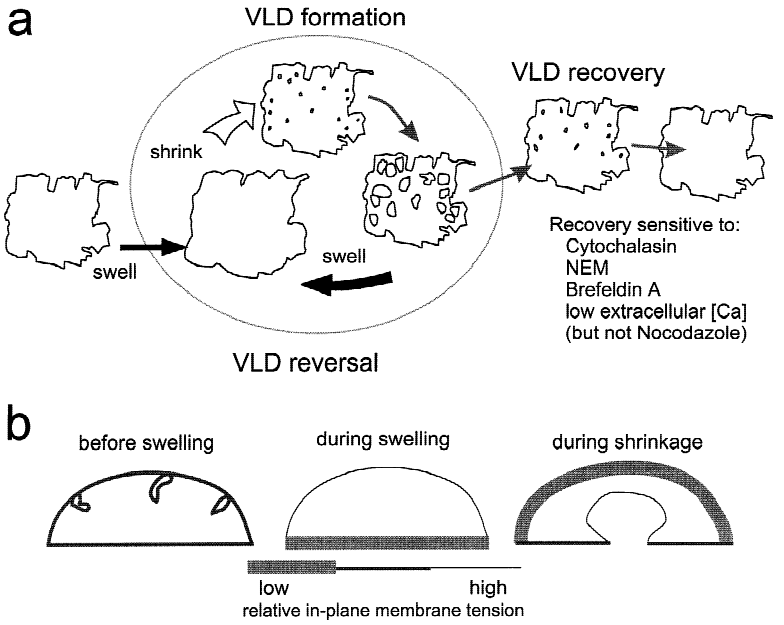

Fig. 1. Vacuole-like dilations (VLDs). (*a*) Scheme showing how VLDs form and reverse or recover in adherent cells, in response to osmomechanical perturbations. As indicated, recovery, but not formation and reversal, is inhibited by drugs (Reuzeau et al., 1995). (*b*) A simplified model of a substratum-adherent neuron showing that regional membrane tension variations in swelling-then-shrinking neurons (Dai et al., 1998) seem to yield a net flow of bilayer (flow is necessarily from low-to-high tension) that dilates the invaginating VLDs. How high tension is generated at VLD initiating sites is, however, unknown. In *a*, the depiction is "from above" (X/Y plane), in *b*, it is in the Z-plane.

~10 μm, presumably driven by membrane tension gradients favoring a flow of bilayer toward VLDs (Fig. 1*b*).

VLDs are normally transient, disappearing by cell-mediated "recovery," but they persist if either actomyosin or membrane trafficking are inhibited (Reuzeau et al., 1995); cytochalasin, N-ethylmaleimide and brefeldin A (but not nocodazole) inhibit VLD recovery. By contrast, VLD formation and VLD reversal, which depend directly on mechanical forces generated by swelling and shrinking, are unaffected (Fig. 1*a*).

Osmotic swelling triggers F-actin rearrangements variously interpreted as depolymerization or disorganization (Ziyadeh, Mills & Kleinzeller, 1992; Cornet, Lambert & Hoffmann, 1993; Cornet, Isobe & Lemanski, 1994; Czekay, Kinne-Saffran & Kinne, 1994; Mills, Schweibert & Stanton, 1994; Morán et al., 1996; Henson et al., 1997). Shrinkage evidently produces the opposite effect. For cells responding to swelling with a regulatory volume decrease (RVD), the cell-mediated shrinkage coincides with rearrangements of F-actin (e.g., Cornet et al., 1994; Henson et al., 1997; Mountain et al., 1998). Neurons can limit their swelling (Strange, 1993); this sometimes but not always amounts to RVD *per se* (Morris, Williams & Sigurdson, 1989; Lippmann et al., 1995; Wan et al., 1995; Morán et al., 1997; Andrew, Lobinowich & Oshehobo, 1997). We elicit VLDs by shrinkage that is not cell-mediated as in RVD, but imposed by bath osmolarity. To what extent any resulting F-actin responses are driven by shrinkage *per se* (*vs.* signaling cascades) is important to ascertain, but calcium at least, is irrelevant since swell/shrink cycles yield negligible calcium perturbations in *Lymnaea* (Herring et al., 1998). Significantly, cell-mediated shrinkage (RVD) in neurons, which is accompanied by F-actin rearrangements, requires no Ca-signaling (Lippmann et al., 1995; Morán et al., 1997). In protoplasts of plant cells (guard cells) that routinely undergo large volume changes, osmotically induced fusion and fission of plasma membrane material is Ca-independent and appears to be modulated by membrane tension (Homann, 1998).

Surprisingly little is known about the joint coordination of cell volume and surface area. Does the cortical cytoskeleton play a role? Using osmotic perturbations, we monitored the disposition of F-actin and surface membrane in neurons undergoing rapid surface area and volume changes. The large-sized molluscan neurons used facilitate visualization of both VLDs (Reuzeau et al., 1995) and of F-actin (Forscher & Smith, 1988; Welnhofer, Zhao & Cohan, 1997) during volume changes and has allowed us to monitor capacitance changes during swelling and shrinking (Wan et al., 1995; Dai et al., 1998). Cytochalasin blocks VLD recovery (Reuzeau et al., 1995) and since recovery includes the pinching off of retrieved membrane as vacuoles (Mills & Morris, 1998), this points to dynamic F-actin as a player in surface area regulation. The fundamental question addressed here is whether F-actin associates directly with newly invaginated membrane and whether VLD-associated F-actin is dynamic.

Materials and Methods

Cells and Solutions

Circumesophageal ganglia dissected from adult snails (*Lymnaea stagnalis*) were placed in normal saline (NS) containing (in mM): 50 NaCl, 1.6 KCl, 3.5 $CaCl_2$, 2.0 $MgCl_2$, 5.0 HEPES, 5.0 glucose; pH adjusted

to 7.6 with 1M NaOH (126 mOsm). Gentamicin was added at 50 μg/mL (NS/G). Ganglia were digested with gentle agitation for 30 min in reduced Ca (0.5 mM $CaCl_2$) NS with 0.25% type XIV protease (Sigma, St. Louis, MO) and washed twice in NS. Neurons were plated on uncoated 22 × 22 mm glass coverslips, number 1 thickness, and cultured in NS/G for 2 days. Plating was accomplished by teasing apart with forceps one ganglion per coverglass, releasing neurons on to untouched glass.

For double coverslip chambers, an oval of sterile silicone grease was syringed on a sterile 24 × 60 mm coverslip. NS/G was added and neurons were plated into the oval and cultured for 2–3 d. For experiments, a 22 × 22 mm glass coverslip was pressed on, leaving a 100–150 μm gap between coverslips. After removing excess solution and grease, dots of molten soft wax (equal parts lanolin, paraffin wax, petroleum jelly) were applied at the corners to secure the two coverslips. Solutions (150–250 μL) were pipetted on at one edge of the resulting flow-through chamber and wicked through at the other edge with tapered strips of filter paper. Solution changes were completed in ~30 sec.

Neurons were hyposmotically swollen by either (i) briefly substituting NS with distilled water as in Reuzeau et al. (1995) for conventional microscopy or (ii) by washing in a 50:50 NS: distilled water solution (all other experiments). A hyperosmotic solution of 3.5 × NS was made by adding sucrose to NS to an osmolarity of 425 mOsm.

For cytochalasin B (CB) experiments, neurons were pre-exposed to 10 μM CB (Sigma, St. Louis, MO) in 0.5% DMSO for 20 min before VLDs were elicited right through until fixation. In controls, the same DMSO concentration was used with no CB. For the rhodamine 123 experiments neurons were exposed to 26 μM rhodamine 123 (Sigma) for 13 min prior to washout and viewing.

All procedures were carried out at room temperature.

Fixation and Staining

Two glutaraldehyde fixation and staining procedures or minor variations of them were used; this has no significance beyond the fact that different protocols were standard in the labs where the work was performed. Three or more slides of each experimental and control treatment were made and viewed. Molluscan neurons have high profiles so cell-bearing coverslips were elevated with greased coverslip chips at the time of mounting.

Procedure 1 (*For Conventional and Confocal Microscopy*)

Neurons were fixed in 0.25% glutaraldehyde in sodium cacodylate buffer. The fixation stock solution was 0.13 g $CaCl_2 \cdot 2H_2O$, 2.38 g sodium cacodylate (BDH Ltd., Poole, UK) added to 180 mL H_2O. Within <2 hr of use, 15 mL of stock was mixed with 1 mL 4% glutaraldehyde (179 mOsm, pH 7.6). NS was exchanged slowly with the fix, then a further 10 min fix was followed by washes (3 × 5 min) in phosphate buffered saline (PBS) and 5 min extraction (0.1% Triton X-100 (Sigma, St. Louis, MO) in PBS). After rewashing (PBS 3 × 5 min) and reducing in 1% sodium borohydride in PBS (3 × 5 min) and another PBS wash, neurons were stained for 30 min in 70 μL of 0.44 μM rhodamine-phalloidin (Molecular Probes, Eugene, OR) in PBS then washed (PBS, 3 × 3 min) and mounted. The mounting medium was 2% n-propyl-gallate in PBS:glycerol (1:3). Coverslips sealed with clear nail polish were kept in the dark at −20°C until viewed the next day.

Procedure 2 (*For High Resolution Microscopy*)

Neurons were fixed in 0.5% glutaraldehyde in PHEM buffer (60 mM PIPES, 25 mM HEPES, 2 mm $MgCl_2$, 10 mm EGTA, pH 6.9) for 2 min, post-fixed in 0.1% glutaraldehyde in PHEM for 20 min, rinsed for 5 min in PHEM, extracted in 0.5% Triton X-100 in PHEM for 5 min, rinsed in PBS 2 × 5 min each, reduced in 0.5% sodium borohydride in PBS for 10 min, rinsed in PBS 2 × 5 min each, incubated in 0.33 μM Bodipy-phallacidin in PBS (1:20 dilution) (Molecular Probes, Eugene, Oregon) for 20 min, 2 × 5 min rinsed in PBS, dipped quickly in distilled water to remove any salts and mounted in Slow-Fade (Molecular Probes, Eugene, OR) and viewed immediately.

Viewing Cells

For conventional microscopy of cells fixed by Procedure 1, neurons were viewed on a Zeiss Axiophot microscope fitted with a 40× (N.A. 0.75) phase contrast/neofluor objective and a filter set consisting of a 546 nm excitation filter, a 580 nm chromatic beam splitter and a 590 nm barrier filter. Photomicrographs were taken on a Zeiss 35 mm camera system using Ilford XP-2 400 ASA and Kodak TMY 400 ASA films. Phase contrast exposure times were automatic and fluorescence exposure times were manual, usually between 30–50 sec.

For confocal microscopy of cells fixed by Procedure 1, cells were viewed and imaged with a Bio-Rad MRC 1024 laser scanning confocal microscope (Hemel Hempstead Herts, UK) using a Krypton-Argon laser. A 60× oil immersion DIC (differential interference contrast) objective (NA 1.4) and a universal oil condenser (NA 0.85) was used on an Olympus IX70 inverted microscope. Each field of view was simultaneously captured in DIC and fluorescence using Lasersharp acquisition software (Bio-Rad, Hemel Hempstead Herts, UK). The laser was used at a laser power of 3% to excite the fluorophore conjugated to phalloidin (either rhodamine or Alexa 568, Molecular Probes, Eugene OR). Appropriate emission/barrier filters were used and images were Kalman filtered online (6 replicates were usually used). Z-stacks and Z-images were obtained using the system's focus motor, beginning at the substratum. For Z-images, the vertical and horizontal pixel sizes were matched to avoid vertical distortion. In some cases, the reflectance interference mode was used to locate the substratum. Images were processed in Confocal Assistant 4.02 (freeware from Bio-Rad for their proprietary ".pic" files); digital filters used were brightness, contrast, gamma, and sharpen. Composite images were generated from selected slices of a Z-series using Confocal Assistant's 3-D projection subroutine in maximum pixel mode. Images were assembled in Corel Photo Paint and Corel Draw.

For cells fixed by Procedure 2, neurons were viewed on an inverted Nikon microscope equipped with a dry condenser (N.A. 0.85) and a 100× (N.A. 1.25) plan 4 objective for phase contrast and fluorescence microscopy. Specimen irradiation was minimized by placing a shutter (Uniblitz, Rochester, NY) in front of the 100 W halogen light and a green interference filter and infrared filter (Chroma Technology, Brattleboro, VT) were inserted into the light path. The shutter was either controlled manually or electronically triggered by a CCD camera controller.

Time-lapse movies were collected with a cooled CCD camera containing a back-illuminated 512 × 512 CCD (TEA/CCD-512, Princeton Instruments, Trenton, NJ) with 16 bit resolution. Microscopy images were projected either 2×, 2.5×, or 4× before acquisition. A computer (Power Macintosh 7100) with a nubus interface was used to control image acquisition. A "movie" script was written with IP Lab Spectrum software (Signal Analytics, Vienna, VA) to control exposure time, time intervals between image acquisition and number of frames in a movie. All image processing included background subtraction. For video-enhanced DIC microscopy, a 100× (N.A. 1.4) plan apo lens and an oil condenser (N.A. 1.4) were used. Specimens were illuminated with light from a 100 W mercury lamp that was passed through a fiber optic scrambler (Technical Video) before entering the transillumination

pathway and were projected 4×. A shutter (Uniblitz, Rochester, NY) was used to minimize specimen irradiation between image acquisition. Video images were obtained with a Newvicon camera (Dage-MTI, Michigan City, IN) and converted to digital images using a computer (Power Macintosh 7100) with a frame grabber (Perceptics PixelPipeline). Time-lapse moves were made as described above. Images were processed in Adobe Photoshop and assembled in Adobe Illustrator.

Testing for Appropriate Fixation

Fixation *per se* can induce artifacts that might be confused with VLDs (e.g., Auer & Coulter, 1994). Preliminary monitoring by Hoffman Modulation (40× objective) showed paraformaldehyde to be unacceptably vacuologenic and methanol/acetone fixation, which was non-vacuologenic, did not preserve F-actin structure in the neurons. Glutaraldehyde at 0.25 or 0.5% were acceptable in *Lymnaea* neurons, though even the lower concentration was sporadically vacuologenic. When glutaraldehyde fixation did vacuolate no-shock control neurons, F-actin was not associated with the vacuoles. No shock control preparations were included and viewed in every batch.

Glutaraldehyde fixation disrupts endomembranes in neural tissue prepared for electron microscopy (Cheng & Reese, 1987). Such disruption might go undetected with transmitted light microscopy, so we examined 0.25% glutaraldehyde fixation at higher resolution. Confocal imaging was used to monitor tubular endoplasmic reticulum stained with the vital endomembrane dye, diO. No fixation-induced rearrangements of the endotubular reticulum were detected. Terasaki et al., (1984, 1986) also found that 0.25% glutaraldehyde preserved the endotubular reticulum. A drawback of glutaraldehyde, its autofluorescence, was diminished with Na borohydride. Neuronal somata had the highest background, but we mostly imaged lamellae and growth cones.

Hyposmotically swollen neurons could not be fixed. By 1 min after return of swollen neurons to NS (when the neurons had nascent VLDs ~1 μ diameter), fixation was possible but fixation-induced vacuoles were not uncommon. At this early stage VLDs were just beginning to invaginate in many cells and so were distinct both by their small size and by their abundant actin. Artifactual vacuoles were large and devoid of F-actin. At 5 min, fixation artifacts were rare. For every batch, no-shock controls were checked and fixation was routinely monitored by Hoffman Modulation. Insofar as it was never vacuologenic for no-shock controls, procedure 1 was preferable to procedure 2.

In all but one protocol (fixation of neurons in hyperosmotic medium, Fig. 8*a*), neurons were in normal saline just prior to fixation.

Microinjection of G-actin

Tetramethylrhodamine-5-iodoacetamide labeled rabbit muscle G-actin (rh-actin) was prepared as outlined in Welnhofer et al., (1997) and diluted by 50% in injection buffer (2 mM PIPES, 0.1 mM ATP, 0.1 mM dithiothreitol, 0.05 mM $MgCl_2$, pH 7) to approximately 3 mg/mL. Glass microelectrodes (AM Systems, Everett, WA) were backfilled with rh-actin and neuronal cell bodies were pressure injected with rh-actin under control of a voltage activated valve (General Valve, Fairfield, NJ). Injected neurons were incubated for ~1 hr prior to imaging. Fluorescent digital images were acquired as described above, except a 3 or 10% neutral density filter was inserted into the epifluorescence light path and a 500 msec exposure was used to reduce photobleaching and photodamage to neurons.

Results

F-actin in Control Neurons

In control neurons (Fig. 2) the dominant F-actin structures were filopodia (Fig. 2*a* arrows) at the leading edges of growth cones and along neurite margins, plus scattered puncta. Higher resolution at the substratum (Fig. 2*b* and *c*) revealed the F-actin network of small randomly oriented F-actin bundles. Although the *Lymnaea* central neurons were diverse in their extent of veil formation and arborization, as previously described (Sigurdson & Morris, 1989), their F-actin patterns were like those of other cultured molluscan (e.g., Forscher & Smith 1988; Welnhofer et al., 1997) and vertebrate (Cornet et al., 1994) neurons fixed in glutaraldehyde.

VLDs and F-actin

The standard protocol to elicit VLDs (Fig. 1*a*) was to swell neurons then shrink them in normal saline (NS). As elsewhere (e.g., Auer & Coulter, 1994), aldehyde fixatives were vacuologenic for swollen neurons (*see* Materials and Methods) so F-actin was imaged only after return to NS. Monitored live, swollen neurons had elevated Brownian motion like that with cytochalasin, but whether this cytoplasmic disruption involved disorganization of intact F-actin *vs.* depolymerization, we could not judge.

Within ~0.5 min of shrinking, VLDs were initiated as point invaginations at the substratum and were fully dilated before 5 min. Figure 3*a* and *b* shows VLDs and F-actin in a 5 min neuron; previous work shows that such neurons undergo full recovery (cell-mediated disappearance of VLDs) by 1–3 hr (e.g., Fig. 4*c* of Reuzeau et al., 1995). Like controls, VLD-bearing neurons had F-actin rich filopodia and puncta. VLD-associated F-actin in Fig. 3*b* typifies the roughly annular profiles just above the substratum and the wide range of F-actin staining intensities at different VLDs. The general relationship between VLD membrane and F-actin was evident in such phase/fluorescence pairs but, with each optic emphasizing different parts of the cell signal, the sizes seldom coincided.

In fact, F-actin annuli were not rings but optical sections through membranous dilations whose 3-dimensional topology is evident in composite confocal images (Fig. 3*c*) in which VLDs appear spheroid or multilobed. VLDs varied widely in F-actin staining intensity but for 5 min neurons did not find evidence of F-actin-free VLDs. The ghostlike transparency of lightly stained VLDs (e.g., double arrowhead, Fig. 3*c*) reveals their 3-dimensional shapes particularly well. VLDs' dynamism is evident when inspecting individual planes from composites. In one small region (near the down-arrow of Fig. 3*c* composite and individual planes, 3–14), for example, two VLDs were evidently fusing (tilted arrow in 3, 5, 10, 12; compare 3 and 5), another VLD was dilated deep in the cytoplasm but fully constricted at the substratum (down arrow; the small dense F-actin spot in 3, 5 opens out by 10 and by 14 is a bi-lobed dilation) and

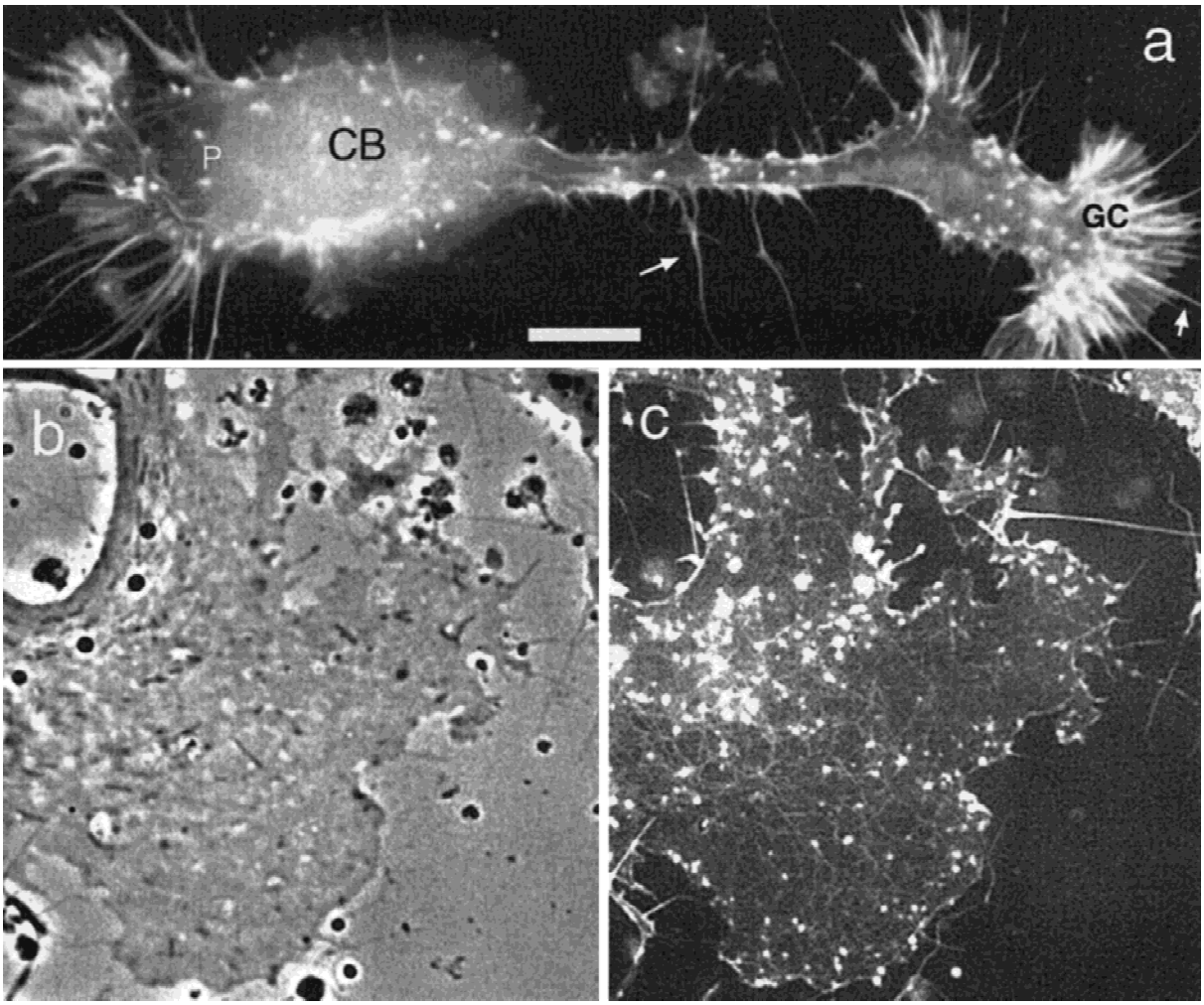

Fig. 2. Neurons stained for F-actin. (*a*) Survey view of a neuron focused near the substratum (conventional epifluorescence, rhodamine-phalloidin). The cell body (CB), a growth cone (GC), filopodia (arrows) and puncta (P) are indicated. For another cell, several protrusions in a veil region are shown in phase contrast (*b*) and fluorescence (*c*) (bodipy-phallicidin); here, not only filopodia and puncta are evident but also the networklike nature of cortical F-actin. Scale: *a* 25 μm; *b* and *c* 7 μm.

finally, another dilated VLD (arrowhead in 12, 14) has no profile near the substratum (i.e., in 3) so may already have pinched off.

F-actin at Nascent VLDs

Although full VLD recovery can take hours, fixation at 5 min would not capture the earliest F-actin changes; in time lapse (Reuzeau et al., 1995) cytoplasmic motions associated with VLD recovery commence almost as soon as VLDs form. We therefore examined neurons when many VLDs were just beginning to invaginate from the substratum, 1–2 min after the onset of shrinking (Fig. 4*a* and *b*). Nascent VLDs, clearly resolvable at ~1 μm diameter, stained densely for F-actin. So soon after having been swollen, some neurons were still prone to fixation-induced vacuolation (*see* Materials and Methods) but VLDs were distinctive: (Fig. 4*c* shows a small F-actin coated VLD surrounded by large fixation-induced vacuoles devoid of F-actin. Optical sectioning showed nascent VLD invaginations to be coated relatively uniformly with F-actin from the substratum to where they ended blindly in the cytoplasm. In spite of their recent cytoplasmic disruption (during swelling), 1–2 min neurons had continuous F-actin strands (filaments or fine bundles); in Fig. 4*b* individual strands exceeding 10 μm in length are evident.

F-actin at the VLD Mouth

Initially (1–2 min), most VLD-bearing neurons showed simple ring F-actin profiles (as in Fig. 4) but by 5 min,

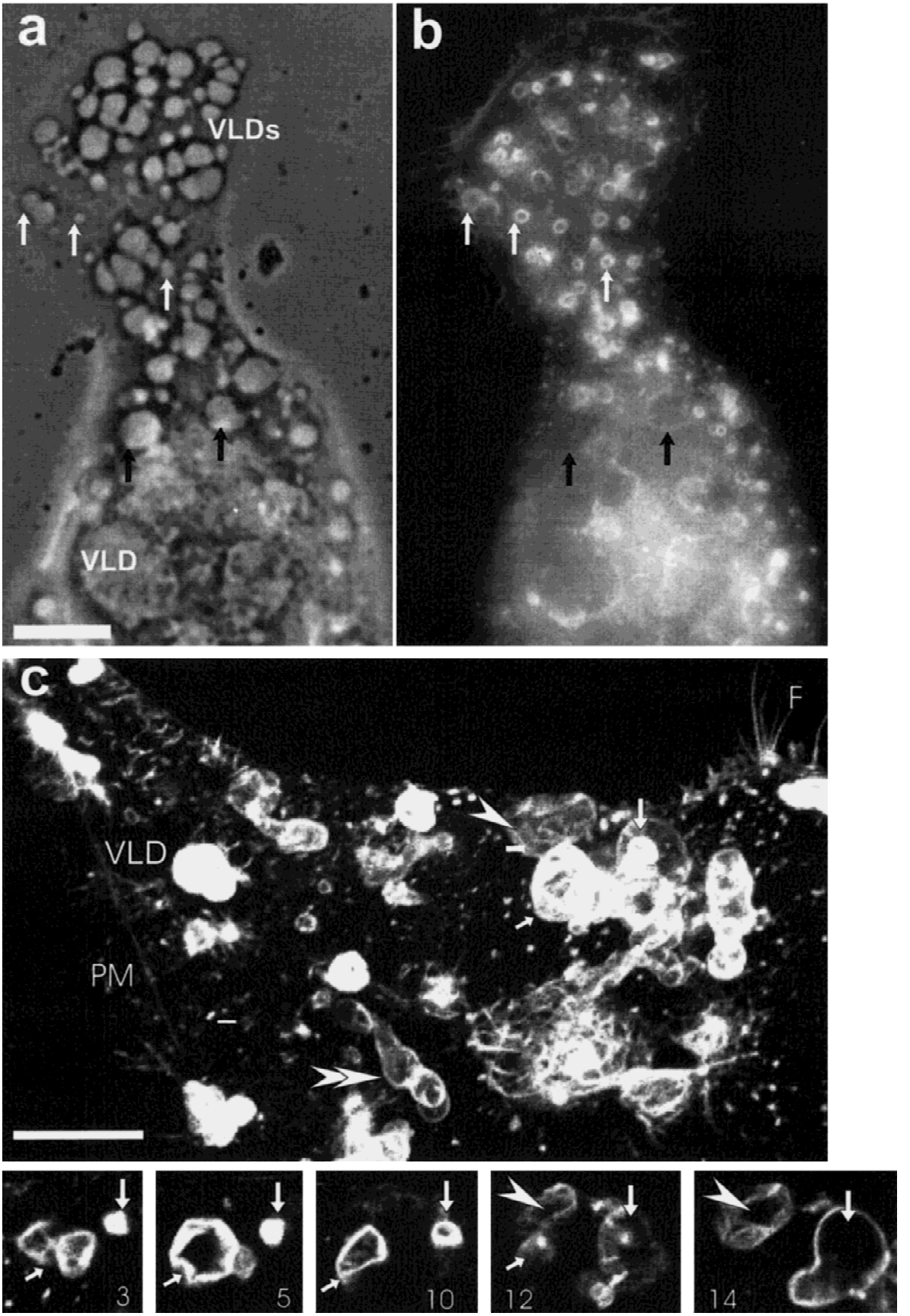

Fig. 3.

VLD F-actin formed complex shaped "mouths" at the substratum (Figs. 5 and 6) consisting, it seemed, of F-actin in lamellipodial and filopodial protrusions. In some unusually actin-rich neurons, VLDs showed much mouths by ~1–2 min (Fig. 5*a*) but by 5 min (Fig. 5*d*) they were universal except at mouths too small for elaborations to be resolved. In high resolution images from 5 min neurons (Fig. 6*a–c*), VLD mouth F-actin strongly resembled "leading edge" F-actin (i.e., that at growth cones or regions of advancing cell margins). This resemblance was highlighted by the diverse *Lymnaea* neuron population studied, since individual neurons' idiosyncratic leading edge characteristics (e.g., frequency and length of filopodia) tended to be reflected in their VLD leading edge characteristics.

Dynamics at the Mouth

To monitor the dynamics of membrane protrusions that formed at the edge of VLDs in live neurons undergoing recovery, we used time-lapse video-enhanced DIC (Fig. 7). Filopodia and lamellipodia formed where VLDs contacted the substratum (Fig. 7*b*) but not above the level of the substratum (Fig. 7*a*). Time-lapse images showed that lamellipodia extended onto the substratum and that filopodia extended, retracted or were swept laterally across the field (Fig. 7*c–g*). As the accompanying graph illustrates, the rates of advance and retraction of processes varied over time, but when filopodia grew steadily, they did so at ~3 μm/min. Over longer time periods, many VLDs began to shrink and disappeared completely during the recovery period. The rate of closure of VLDs measured from DIC images was 0.7 ± 0.3 μm/min (n = 12).

Fluorescent G-actin Accumulates at VLD Edges

To study temporal aspects of F-actin reorganization at VLDs in live neurons, we injected *Lymnaea* neurons with rhodamine-labeled G-actin (rh-actin) (Fig. 8), an approach we have used to monitor F-actin dynamics in *Helisoma* growth cones (Welnhofer et al., 1997). In several cases, such as Fig. 8, good incorporation of the labeled actin was achieved. Though initially devoid of filopodia, this neuron showed puncta and a filamentous actin network. Within 0.5 min of switching to swelling medium and throughout the swelling period, the actin network became less visible, perhaps because swelling decreased the rh-actin concentration. Additionally, actin filaments may have been lost in response to swelling. However, within 5 min after returning to NS (eliciting VLDs), fluorescence was localized to peri-VLD regions (Fig. 8*b*), precisely as expected from F-actin localization in fixed preparations. Two possible interpretations are that *de novo* polymerization of F-actin occurred at VLDs, and/or that dispersed F-actin filaments reorganized. There was also increased actin fluorescence at cell margins, suggesting increased actin assembly at lamellipodial edges.

Rh-actin fluorescence at the periphery of VLDs was not uniform; high intensity fluorescence appearing at the mouth corresponded to areas of extended lamellipodia and filopodia (Fig. 8*c–f*), indicating incorporation of rh-actin by these structures as actin filaments assembled and disassembled at different leading edge locations. In sequential time-lapse images (Fig. 8*g–j*), rh-actin fluorescence intensity varied in position and width and correlated with the formation of membrane protrusions. This dynamism prevented quantification of actin filaments surrounding VLDs. As VLDs closed during recovery, rh-actin fluorescence dispersed at about the same time that the phase-contrast image of the VLD disappeared (Fig. 8*g′–j′*). This indicated that VLD closure was associated with disassembly or reorganization of actin filaments.

VLD recovery, as seen here, was normal in G-actin-injected neurons. By 15 min, about half the VLDs and associated F-actin present at 5 min had disappeared. By 80 min, most VLDs were gone and labeled G-actin was associated mostly with puncta and the fine F-actin network. F-actin puncta were dynamic, decreasing in number during swelling, reappearing as VLDs formed (Fig. 8*b*) then increasing in number as recovery progressed. These experiments directly corroborated findings from fixed neurons stained for F-actin, namely that F-actin rapidly localizes around newly formed VLDs.

The F-Actin Network at VLDs

Although in bright field microscopy, VLD dilations can look like unadorned lipid bilayer bubbles, Figs. 3*c*, 5*b,c*, and *e*, show them to have a complete F-actin coating. F-actin structures at VLD mouths were thin (in the Z-plane), usually giving way to the dilated F-actin coat <1

Fig. 3. VLD-bearing neurons stained for F-actin. (*a* and *b*) Conventional epifluorescence, rhodamine-phalloidin, fixation at 5 min, compares phase (*a*) and corresponding fluorescence (*b*) images (focus ≤1 μm from the substratum); arrows colocate 5 VLDs. VLDs (*a*) appear larger in phase than expected from the corresponding fluorescent (*b*) rings. Staining intensity differed among VLDs (e.g., compare among VLDs with arrows). (*c*) A composite confocal fluorescence image (Alexa 568 phalloidin, fixation at 5 min, 35-step Z-series, 0.5 μm/step). In such 3-D images, lightly stained VLDs (double arrowhead) revealed more structure than intensely stained ones (VLD). Where the plasma membrane was perpendicular to the confocal plane, its cortical F-actin is evident (PM). Filopodia (F) and scattered puncta were evident. Bottom panel, *c*: VLDs at various levels through this image stack, numbers refer to step up from substratum. Particular VLDs (*see text*) are located by arrows and arrowhead in composite and bottom panel. Scales: *a,b* 20 μm; *c* 10 μm.

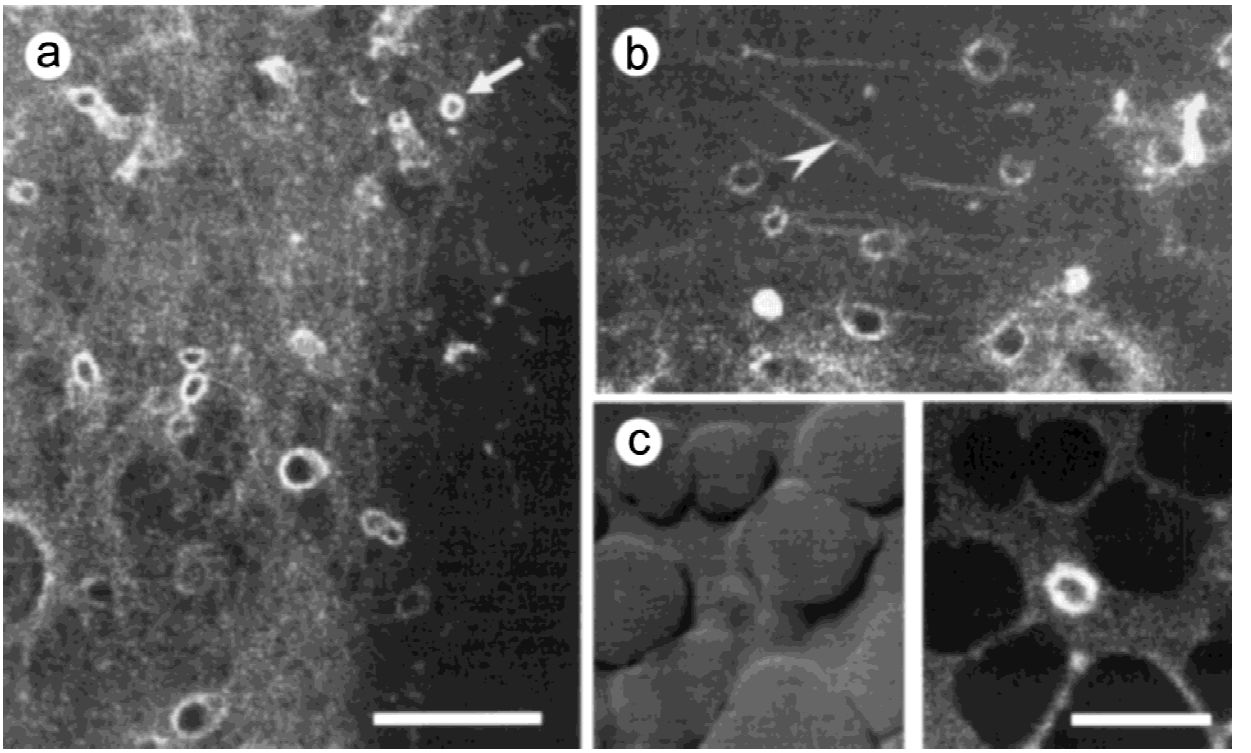

Fig. 4. Confocal images of nascent VLDs. Fixation was 1–2 min after swollen neurons returned to NS (rhodamine-phalloidin). (*a*) Small F-actin coated VLDs (arrow). (*b*) Similar to *a*, and showing distinct F-actin strands (arrowhead). (*c*) DIC, fluorescence pair; in the center is a nascent F-actin coated VLD surrounded by fixation induced vacuoles without F-actin. Scales: *a*,*b* (in *a*) 10 μm; *c* 6 μm.

μm above the substratum. High resolution phase contrast/fluorescence images of VLDs (Fig. 9*a–c*) at 5 min reveal details of the cortical F-actin network and suggest that some of the F-actin forming the general cortical cytoskeleton at the substratum (*see* Fig. 9*b*) invaginated (Fig. 9*c* is deeper in the cytoplasm) along with invaginating VLD bilayer. During this process, however, some of the F-actin, rather than being carried along with the invaginating and dilating membrane, evidently became reoriented or assembled to create the motile VLD mouth.

Live-cell experiments showing bath-dye retention by VLDs after washout (Mills & Morris, 1998) show that during recovery some VLDs invaginations become vacuoles, while others remain patent. Vacuolization (= "retrieval" or "reinternalization") requires full constriction of the VLD mouth; constriction completed or in progress was seen (Fig. 3*c* sections Fig. 5*e* and *f*) wherever F-actin profiles pinched off at or above the substratum. Consistent with live cell findings, constricted VLDs were frequently immediately adjacent to still-patent ones. Constriction might be achieved by centripetal advance of the VLD leading edge and/or by a nooselike tightening of an actomyosin ring. Perhaps intensely stained VLDs (e.g., arrows in Fig. 9*e* and *f*; *e* confirms these as VLDs, not puncta) reflected a compaction of F-actin related to the constriction process.

F-actin Rearrangements at VLDs are Mechanically Triggered

The mechanical (not the chemical) component of osmotic shrinkage is what elicits VLDs (Reuzeau et al., 1995). Mechanical effects alone (i.e., shrinkage) may not, however, trigger F-actin rearrangements at VLDs; swelling-induced effects (F-actin depolymerization, disruption or proteolysis (*see* Ziv & Spira, 1998)) might be necessary preliminaries. The routine protocol for eliciting VLDs was "swell-then-shrink in NS" since this allowed shrinkage, VLD formation and VLD recovery all to occur in NS, but the critical step is shrinkage *per se* (*see* Reuzeau et al., 1995) since large hyperosmotic stimuli alone induce VLDs. The effects of shrinkage alone on F-actin were determined by eliciting VLDs with 3.5 × NS (sucrose added to NS) for 5 min. This generated multiple VLDs in all neurons (e.g., Fig. 10*a*, phase). As Fig. 10*a* (fluorescence) demonstrates, prior swelling was unnecessary for F-actin reconfiguration at VLD mouths. The VLDs and their associated F-actin (at the substratum, Fig. 10*a*, and, not shown, coating the dilation regions) were qualitatively indistinguishable from those elicited by swell/shrink. This argues that the trigger for F-actin rearrangements at VLDs was primarily mechanical (i.e., related to forces produced during shrinkage)

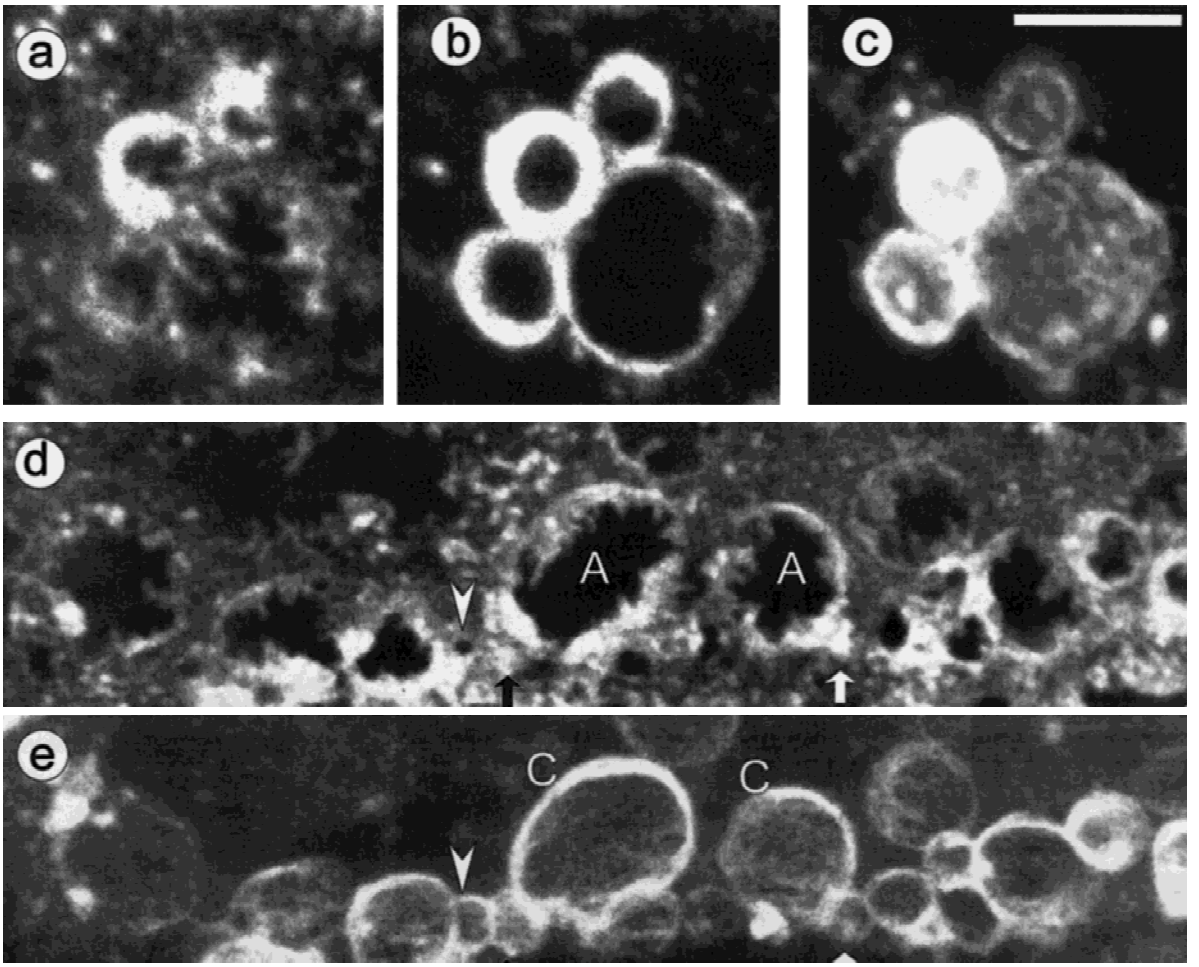

Fig. 5. Confocal Z-series images of F-actin at VLDs. Neurons were fixed at 1–2 min (*a–c*) or 5 min (*d,e*) after VLD initiation (Alexa 568 phalloidin). The set *a–c* shows 4 adjacent VLDs at the substratum (*a*, composite, steps 1–2 in a 0.5 μm/step Z-series), the midrange (*b*, composite, steps 3–6), and the tops (*c*, composite, steps 7–14). These VLDs were unusually advanced for 1–2 min. The set *d,e* shows the substratum (*d*, composite, steps 1–2, 0.3 μm/step Z series) and middle-plus-top (*e*, composite, steps 5–18) of many VLDs; two VLDs mouths (A) and, above, their F-actin coatings (C), are indicate. A VLD with an almost closed mouth (arrowhead, compare *d,e*) and two with mouths fully constricted (black and white arrows) are indicated. Scales: *a–c* 5μm; *d,e* 10 μm.

rather than chemical in nature. In fact, mechanical forces may not only have triggered but provided the motive force for some of the F-actin rearrangements.

F-actin after VLD Reversal

When VLD-bearing neurons are forced to reswell, their VLDs reverse (shrink and disappear) within minutes (*see* Fig. 1*a*). This reversal (like VLD formation) is driven by exogenous mechanical forces, and thus differs from the cell-mediated (cytochalasin-sensitive) process of recovery (Reuzeau et al., 1995). We wished to examine F-actin immediately after VLD reversal (would there be F-actin "ghosts" left behind in the cytoplasm?), but because hyposmotically swollen neurons do not tolerate fixation, VLDs were formed using hyperosmotic medium (3.5 × NS as in Fig. 10*a*) and neurons were then "swollen" in NS to cause VLD reversal (as in Reuzeau et al., 1995). Full reversal of VLDs required ~4 min (monitored by Hoffmann optics), at which point neurons were fixed and stained. As seen in Fig. 10*b* VLD-associated F-actin configurations disappeared along with the VLDs.

An advantage of reversing in NS (as opposed to the standard protocol, involving swelling in hyposmotic saline) is that the observed outcome — loss of the F-actin associated with VLDs — could not be attributed to hypotonicity-induced depolymerization (or reorganization) of F-actin, as might be argued for reversal carried out by swelling in, say 50% medium. Thus, the swelling-

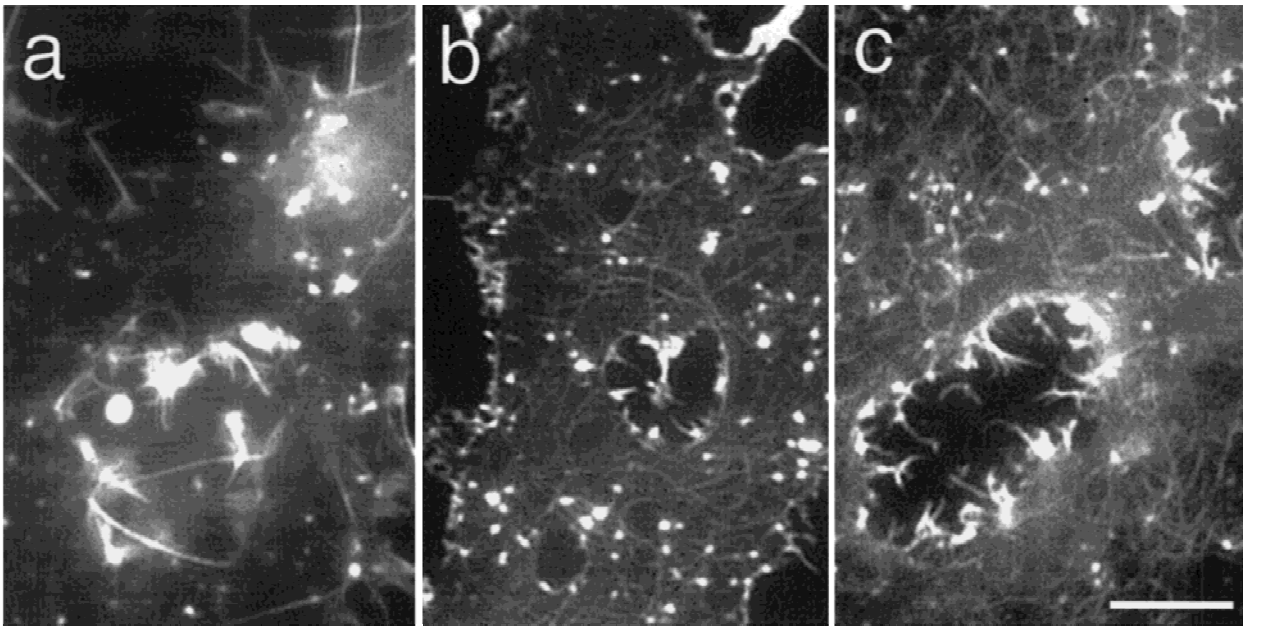

Fig. 6. High resolution images of VLD leading edge (fluorescence, bodipy-phallicidin). Three neurons (*a,b,c*) fixed ~5 min after VLD initiation are shown. Individual processes in VLD leading edge are centripetally arranged and are discrete from the surrounding network of F-actin filaments (*b* and *c*). VLD leading edge in each neuron is similar in pattern to the F-actin at the cell margins. Scale: 5 μm.

induced disappearance of annular F-actin profiles was probably triggered and/or driven by the same mechanical forces that caused VLD reversal.

Effects of Cytochalasin

VLDs' formation is unaffected by cytochalasin B, but their ensuing recovery is blocked (Reuzeau et al., 1995). To directly establish whether this is an F-actin-related effect of cytochalasin, the reagents' effects on F-actin distribution were examined before and after VLD formation (a swell/shrink protocol was used as in Fig. 3). Neurons maintained their adhesion during cytochalasin B (CB) treatment. In CB-treated no-shock controls (Fig. 11*a*), two standard CB effects were evident: extensive depolymerization and/or collapse of filopodial F-actin and the appearance of large intensely fluorescent puncta where F-actin would normally form a filamentous network. As in no-CB controls (i.e., no CB but shocked to elicit VLDs), CB-treated neurons produced abundant VLDs (Fig. 11*b*), but at 5 min, when control VLD mouths would be complex-shaped, CB mouths were conspicuously smooth-lipped. Moreover, the peri-VLD region never showed ring profiles of phalloidin-positive material (F-actin) either at the mouth or coating the dilations. Even "CB-puncta" in close proximity to VLDs appeared to be unrelated to the VLDs. These CB effects confirm that VLD formation (invagination) required no associated F-actin and show that reorganization of F-actin at VLDs was secondary to invagination. Moreover, the smooth-lipped CB-VLDs confirmed that F-actin motility and/or contractility produced the complex-shaped mouths of normal VLDs. Controls for DMSO (shock and no shock; *not shown*) indicated that 0.5% DMSO, used to solubilize CB, did not produce effects on its own.

Nocodazole, which impairs the other major motor protein system — the microtubules — does not inhibit recovery (Reuzeau et al., 1995). 10 μM nocodazole did not affect F-actin distribution during or after VLD formation (*not shown*).

Cell-Mediated VLDs

If VLDs and their F-actin reflect the machinery of surface area regulation operating on "overload" after exaggerated cell volume changes, then cell-mediated VLDs are to be expected when neurons mediate their own shrinkage during the course of, say, regulatory volume decrease or neurite retraction. We noted that when DIC images of fixed control neurons (no osmotic perturbation) had membrane invaginations (Fig. 12*a*), they coincided with F-actin (Fig. 12*b*). These spontaneous structures may correspond to the "dynamic vacuoles" of vertebrate neuron exploratory growth cones thought to be retrieving excess membrane (Dailey & Bridgman, 1993). In older (or overdigested) cultures, vacuoles proliferate,

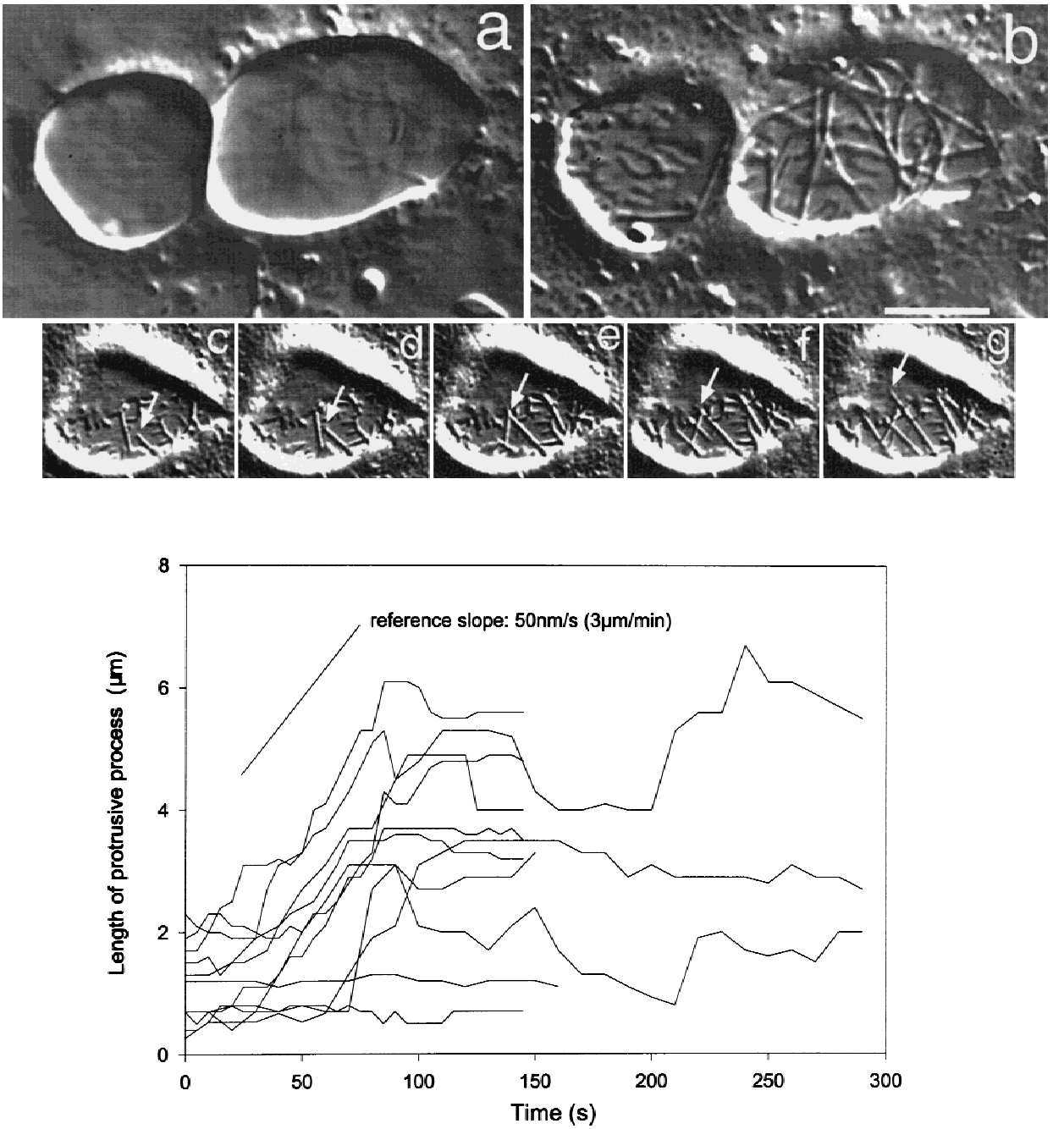

Fig. 7. Video-enhanced DIC microscopy of leading edges of VLDs. Above the substratum (*a*) dilated regions of two VLDs are in focus, while at the substratum (*b*) leading edge processes (lamellipodia and filopodia) of the VLDs become evident. Leading edge dynamics are seen in time-lapse series (~1 hr after VLDs were elicited; (*c–g*) 20 sec intervals). Arrow denotes extension of a filopodium. A graph of the length of filopodia and lamellipodia *vs.* time, made from the three VLDs shown illustrates that the maximum filopodial extension rate ~3 μm/min. Scale: *a,b* 10 μm; *c–g* 17 μm.

perhaps because membrane invagination is followed by impaired reprocessing steps. Fig. 12*c–e* shows a membrane invagination monitored in a live neuron from a relatively old (6 days) culture; its dynamic irregular phase dark coating was probably F-actin-rich but its activity proved ineffectual in constricting the VLD mouth and reinternalizing the membrane.

Reuzeau et al., (1995; Materials and Methods) noted that, paradoxically, prolonged hyposmia (30% medium) elicited VLDs. We confirmed this (Fig. 13) by exposing

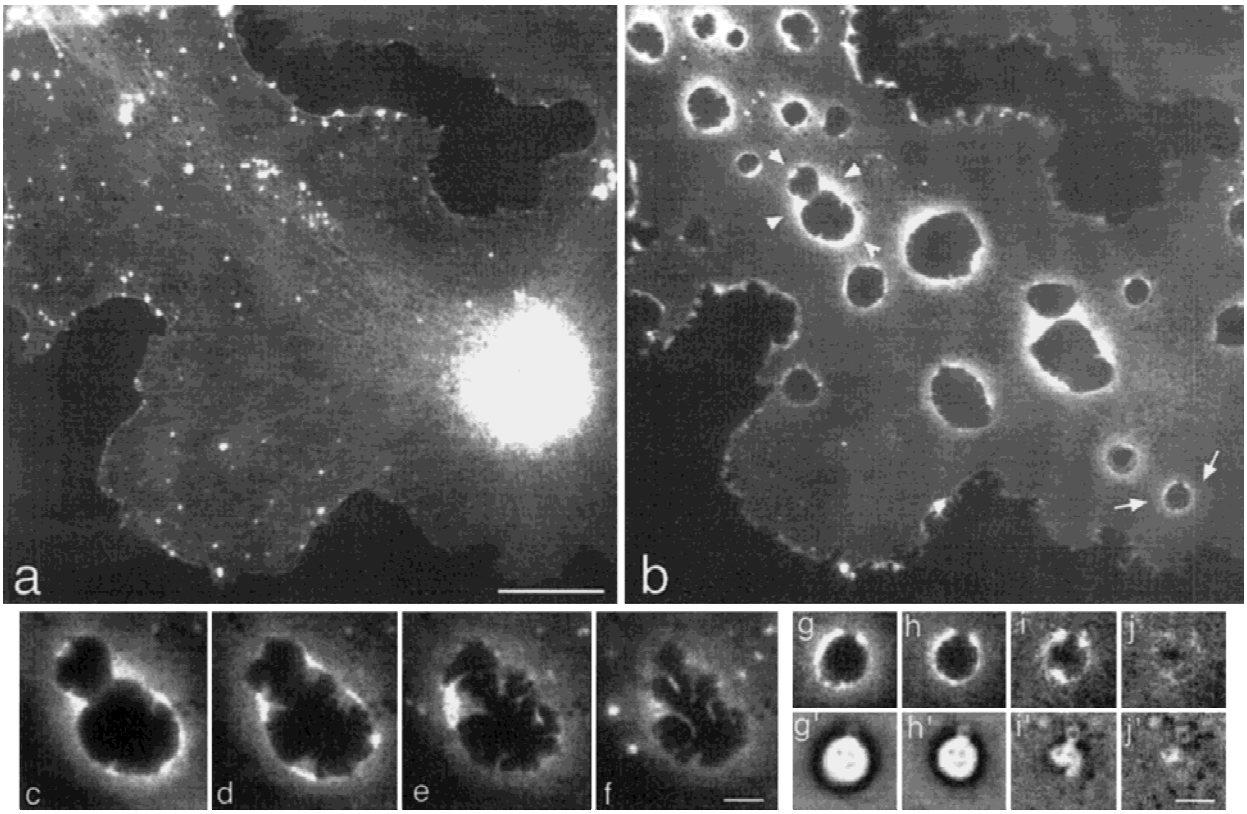

Fig. 8. Reorganization of rh-actin in live neurons after VLD formation, (*a*) ~2 hr post-microinjection, rh-labeled G-actin incorporated into the cytoskeletal network and puncta in the lamellae; 8 min after the swell/shrink perturbation (*b*), rh-labeled actin was enriched around the VLDs and in protrusions along the leading edge of the lamellae. During VLD recovery (followed for the bi-lobed VLD marked by arrowheads in *b*), rh-labeled actin distribution changed with time (*c–f*; 8, 12, 21 and 46 min post-swell/shrink perturbation, respectively). Changes in distribution of rh-labeled actin and in corresponding phase contrast micrographs (*g–j* and *g′–j′*) are shown during recovery of the VLD marked by arrows in *b* at various times after the swell/shrink perturbation: ((*g*,*g′*) 8, (*h*,*h′*) 9, (*i*,*i′*) 10 and (*j*,*j′*) 11 min. Scales: 10 μm in *a* for *a*,*b*; 2 μm in *f* and *j′* for *c–f* and *g′–j′*, respectively.

neurons to hyposmia (50% medium) for 2 hr in flow-through chambers ($n = 3$ cultures). Neurons developed small (<5 μm diameter) VLDs after ~15–60 min. VLD appearance coincided with cell margin retraction (compare Fig. 13*a–c*) suggesting that cell volume was decreasing. If the neurons were undergoing cell-mediated shrinkage as the VLDs formed during prolonged hyposmia, then this would not, after all, be paradoxical, but consistent with shrinkage-induced VLD formation. The video showed the VLDs to be dynamic, but neurons in 50% medium could not be fixed (fixation was vacuologenic) to test for F-actin at the VLDs.

Discussion

Overview: F-actin Associated with VLDs

When made to abruptly shrink, neurons invaginated membrane at the substratum, forming vacuole-like dilations (VLDs); 1–2 min later, VLD membranes were coated with F-actin. Newly invaginated membrane, thus, possessed a cortical cytoskeleton. By 5 min VLDs had mouths at the substratum that were rings of F-actin-rich "leading edge" (lamellipodia plus filopodia). In a growth cone, leading edge is an advancing front whereas VLD leading edge advanced centripetally, towards the center of the VLD mouth (Fig. 14). This action could constrict and reinternalize invaginated VLD membrane.

Cytochalasin-treated neurons formed VLDs lacking both the F-actin coating and a ring of leading edge, confirming that F-actin is not implicated in VLD invagination. But VLDs are transient (they undergo "recovery") and since cytochalasin blocks VLD recovery (Reuzeau et al., 1995), the cytochalasin experiments showed that VLD-associated F-actin contributes to reprocessing of VLD membrane. How (or if) it contributes other than by constriction of the mouth remains to be determined. Since Brefeldin A inhibition of recovery implicates endocytosis (Reuzeau et al., 1995), a novel idea is that contraction of the VLD cytoskeleton may lower in-

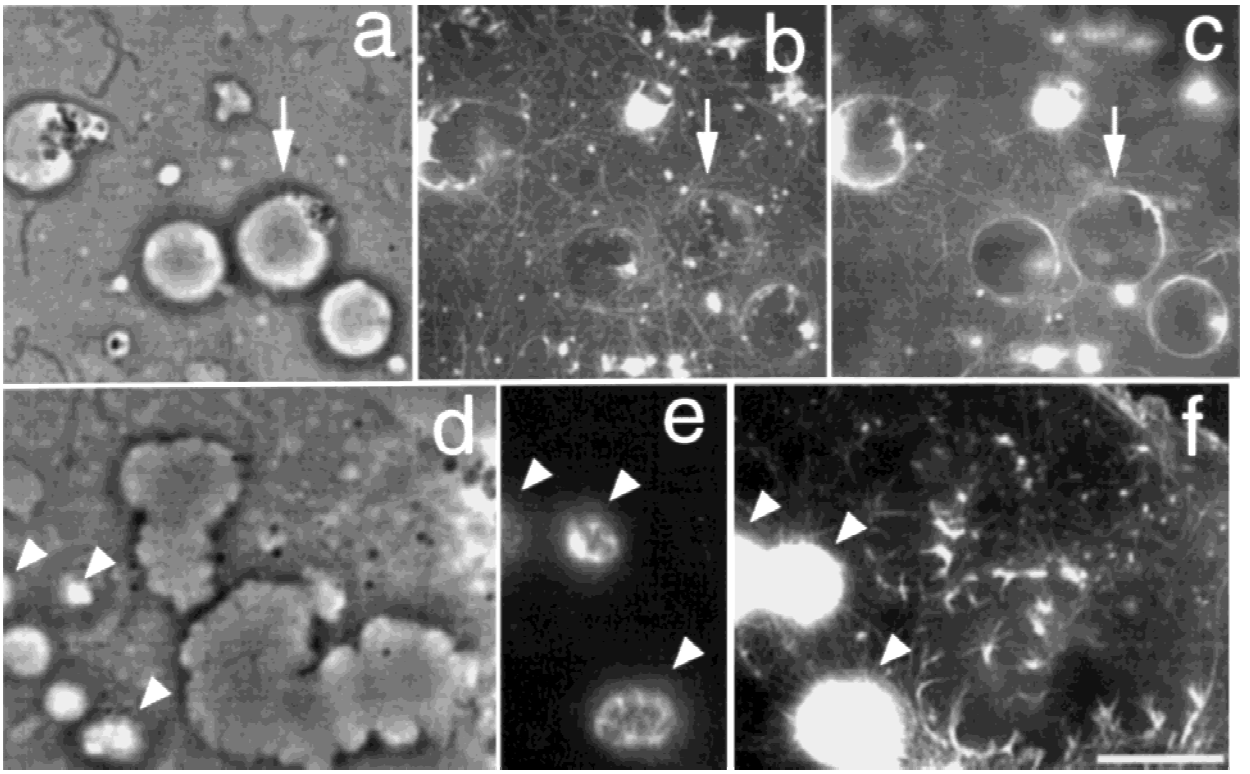

Fig. 9. High resolution images of VLDs and associated F-actin (phase contrast fluorescence pairs, bodipy phallicidin). Two neurons (*a–c, d–f*) fixed 5 min after VLD initiation are shown. Phase images (*a* and *d*), at the substratum, show VLD locations and shapes and paired fluorescence (*b,c,e,f*) colocalizes the F-actin. An arrow in cell *a–c* indicates the same VLD. The mouth (*b*) of this lightly stained VLD (plus mouths of the two adjacent VLDs) appears to be constructed of reorganized F-actin strands from the cortex. Above the substratum (*c*), F-actin provided an uninterrupted coating for the rounded membrane dilation. (*d–f*) Illustrates that neighboring VLDs can have both extreme F-actin density (and mouth shape) differences. Resolving mouth configurations both at intensely (arrowheads, *d,e,f*) and faintly fluorescent VLDs (in *d* and *f*) required different exposure settings (*e vs. f*). Scale: 5 μm.

plane membrane tension thus facilitating endocytosis (e.g., Dai & Sheetz, 1995) of VLD membrane.

Both fixed and live-cell experiments revealed that F-actin rapidly reorganized at VLDs following shrinkage. The absolute osmotic pressure was unimportant; VLDs had F-actin coats and a ring of leading edge at their mouth by 5 min whether neurons shrank in normal or hyperosmotic medium. When reversal was subsequently elicited by swelling, the VLD-associated F-actin configurations disappeared by 4 min. Thus, during two rapid (minutes) mechanically driven membrane events — VLD formation and reversal — both VLD membrane and the peri-VLD cytoskeleton were dynamic.

Invaginating VLD membrane, we presume (Figs. 1*b*, 14), is drawn into the shrinking cytoplasm because this reduces elevated membrane tensions at substratum VLD initiation sites (*see* Mills & Morris, 1998); specifics of the interplay of adhesion and cytoplasmic shrinkage remain to be elucidated. During recovery, VLDs as entities disappear via cytochalasin-sensitive processes, suggesting that mechanical forces generated by actomyosin are involved in relocating membrane. Thus, for recovery, force is endogenously supplied whereas for both VLD formation and reversal, it is exogenous.

F-ACTIN DURING VLD DYNAMICS

Our finding that exogenous forces quickly (<5 min) elicited a concerted remodeling of the actin cytoskeleton and associated membrane is noteworthy given the importance of external forces in establishing neuronal morphology (van Essen, 1997). Membrane invagination (VLD formation) under the influence of shrinking forces, membrane evagination (VLD reversal) under the influence of swelling forces, and F-actin reorganization were so closely coupled that it seems inescapable that the cytoskeleton was responding to the same local forces as the invaginating/evaginating bilayer. If, as suggested by the intense staining of nascent VLDs, VLDs are F-actin coated from the outset, then existing membrane skeleton may be passively drawn inward with invaginating membrane. G-actin can, however, interact strongly with membrane lipids (Bouchard et al., 1998) so additional

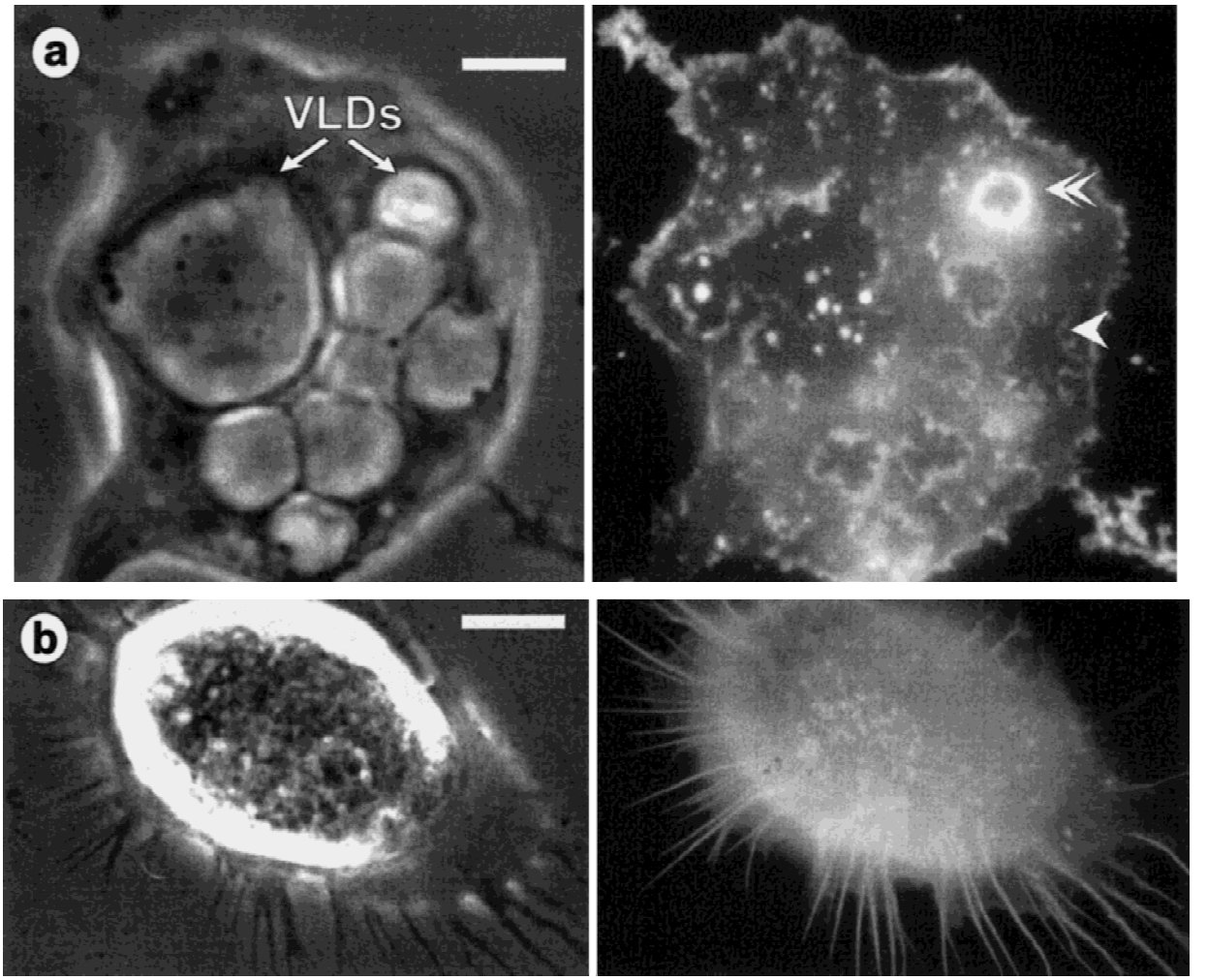

Fig. 10. Effects of shrinkage alone and of reversal (conventional microscopy, phase contrast/fluorescence pairs, rhodamine-phalloidin). (*a*) A hyperosmotically shocked neuron focused at the substratum. The fixation procedure was not changed. VLDs (phase contrast) have leading edges (arrowheads, fluorescence) of different staining intensities. (*b*) A neuron after reversal of VLDs (*see* text for details). Filopodia are normal-looking and abundant at the cell margin; there is no evidence of F-actin formerly associated with VLDs. Scales: *a* 5 μm; *b* 15 μm.

physical processes may augment the coating of invaginating membrane. Whether further F-actin reorganization (e.g., contraction of the network) occurred over the membranous dilation of VLDs is unknown, but at the substratum, VLD mouth F-actin realigned and/or reassembled to yield characteristic centripetally directed protrusive structures.

Thus, an F-actin cortex not only persisted as membrane was drawn back and forth but, at least near the substratum/VLD interface, the actin cortex became more robust and motile and/or contractile. At invagination points, stresses experienced would include bending and extension. Put another way, membrane cytoskeleton became fortified and active precisely where bilayer was subjected to stress. This interpretation coincides with other emerging findings about the mechanoprotective role of the cortical cytoskeleton (Rivero et al., 1996; Zhang, Larsen & Lieberman, 1997; Glogauer et al., 1998).

The density of VLD F-actin varied greatly. Differences at immediately neighboring VLDs may correlate with the finding (Mills & Morris, 1998) that during recovery, some VLDs constrict at the substratum, thereby vacuolating, while immediate neighbors do not. Dense VLD F-actin could indicate contraction, suggesting that constriction had begun prior to fixation. Notably, dense F-actin was seldom a feature of large-mouthed VLDs.

During reversal (elicited by swelling) both VLD bilayer and F-actin were rapidly redistributed, presumably joining the general plasma membrane. For a swelling cell, the redeployment of invaginated cortical cytoskeleton back to more highly stressed surface membrane would seem an appropriate strategy, simultaneously pro-

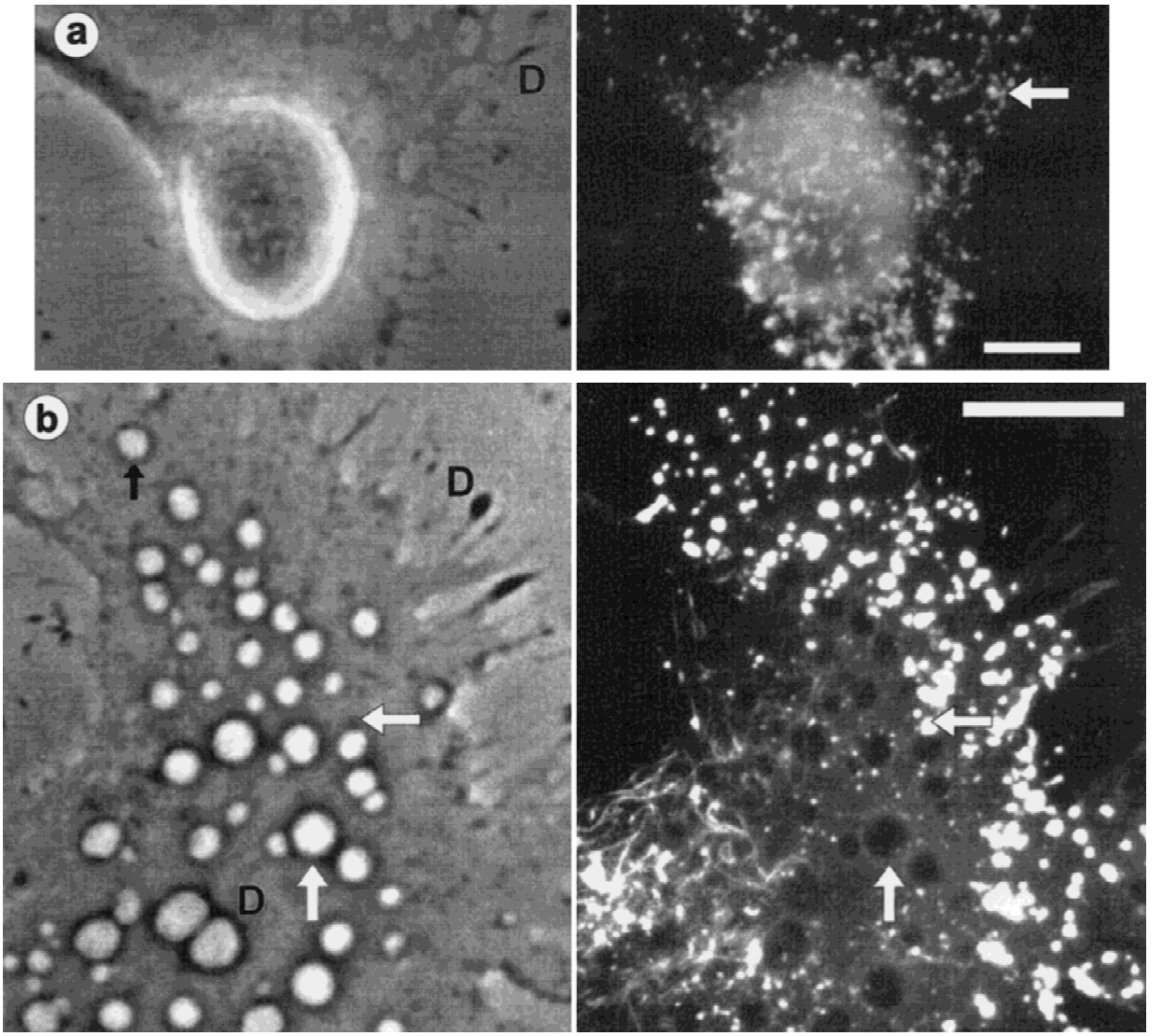

Fig. 11. Effects of 10 μm cytochalasin B (CB) (conventional microscopy, phase contrast fluorescence pairs, rhodamine-phalloidin, 5 min fixation). (*a*) A CB-treated neuron, no VLD-eliciting shock (i.e., CB control). General cellular morphology (phase contrast) was maintained but F-actin (fluorescence) was absent from filopodia in spite of sporadic phase dark (D) material. In veils, phalloidin-positive CB-resistant puncta (arrow) were abundant. (*b*) A CB-treated neuron after a swell/shrink stimulus shows abundant VLDs which lacked F-actin, though CB-resistant F-actin puncta persisted. As in CB controls, phase dark regions (*see* D and vertical white arrow pair) were unrelated to phalloidin-staining. Though some VLDs (e.g., black arrow, horizontal white arrow pair) were located close to phalloidin-positive puncta, there was no evident relationship. Scales: *a* 10 μm; *b* 20 μm.

viding mechanoprotection of the bilayer and surface area regulation.

In swollen neurons, membrane tension is increased (Dai et al., 1998), there is no measurable weakening of the F-actin rich cortex (Lin et al., 1995) and neurite outgrowth is promoted (Bray et al., 1991; Lin et al., 1995). In nascent VLDs, membrane was presumably under elevated tension so it is notable that this membrane's cytoskeleton was at least as robust-looking as that in the general plasma membrane. Swelling neurons undergo N-ethylmaleimide-sensitive writhing (Wan et al., 1995), suggesting that the actomyosin cortical cytoskeleton becomes contractile, counteracting elevated membrane tension. An interesting possibility, therefore, and one consistent with the N-ethylmaleimide-sensitive writhing of recovering VLDs (Reuzeau et al., 1995), is that during recovery, the VLD cytoskeleton contracts, lowering VLD membrane tension, thereby promoting endocytosis.

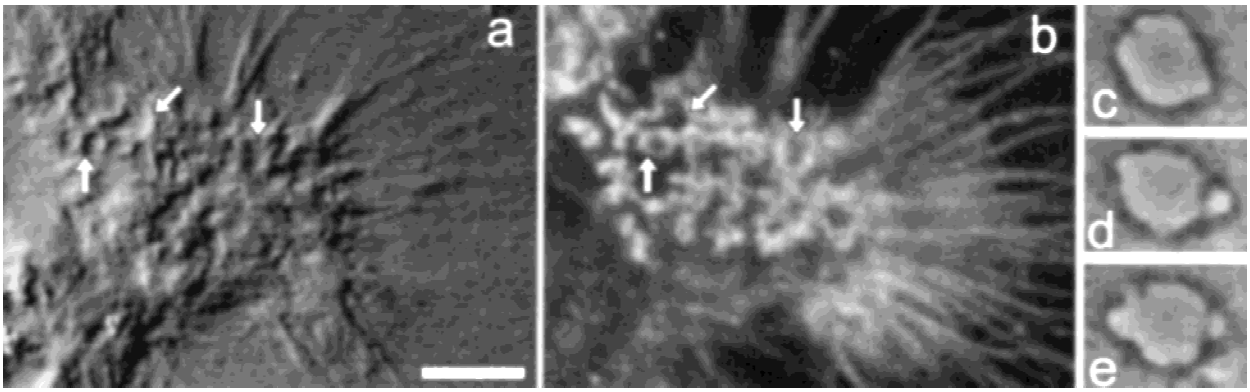

Fig. 12. Spontaneous VLDs. (*a* and *b*) Confocal microscopy, DIC, fluorescence pair; a growth cone in a fixed control neuron; arrows indicate three of several areas where membrane invaginations (*see* DIC) correspond to irregular F-actin rings. (*see* fluorescence). (*c–e*) (Live neuron, phase contrast) a VLD in a control neuron over a 16-min period. Scale: *a,b* 6 μm; *c–e* 7 μm).

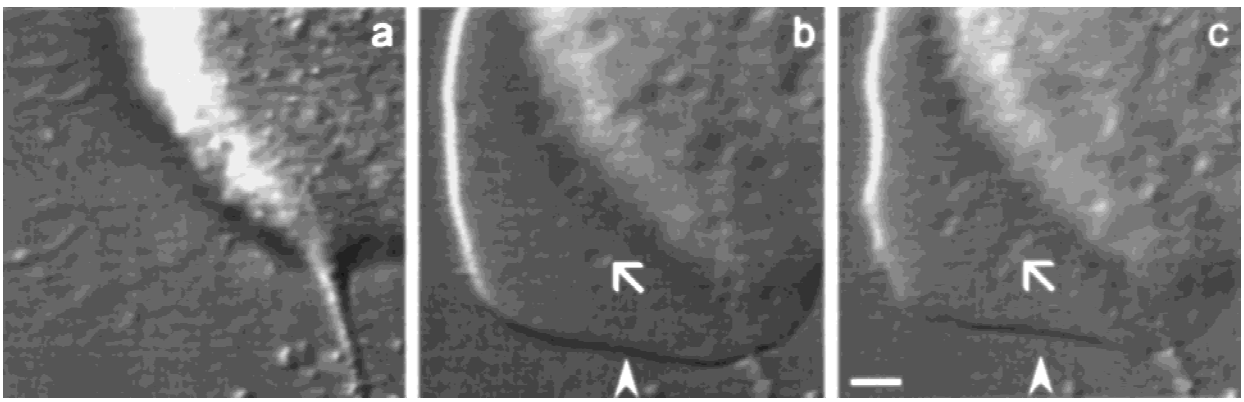

Fig. 13. VLDs during hyposmia. (Hoffman Modulation optics, videotape images, live neuron). VLDs are seen forming during prolonged hyposmia (*a* in NS, *b* in 50% NS for 60 min, *c* in 50% NS for 70 min). Debris at base of *a–c* provides fiducial mark. VLDs (e.g., arrow) are evident (*b*) in the veil and beneath the soma. More are seen 10 min later (*c*), at which time the veil edge (arrowheads, *b,c*) had retracted and was less bloated. Scale: 10 μm.

VLD Mouths Compared to Growth Cones

Growth cone leading edge, like VLD leading edge, has a dynamic mix of filopodia and lamellipodia. The growth rate for steadily elongating VLD filopodia, ~3 μm/min, was not unusual, being ~2× the *average* rates in grasshopper (~1.5 μm/min; Myers & Bastiani, 1993) and *Aplysia* neurons (1.2–1.7 μm/min; Wu & Goldberg, 1993). Except for the obvious topological constraint of being an annulus on a plane, a VLD leading edge could presumably advance like a growth cone (*see* cartoon inset in Fig. 14 "3-D" where this constraint is relaxed). In fact, the rate of VLD advance is almost identical to the rate of growth cone advance of 0.33 μm/min (i.e., ~20 μm/hr (Cohan, 1990)). VLDs closed at 0.7 μm/min, so assuming they closed symmetrically the rate per edge is 0.35 μm/min. In Fig. 14 we propose that there is a commonality in the mechanical forces that elicit VLD leading edge formation (and subsequent activity) and those that promote the formation and subsequent motility of growth cones. Neurite elongation requires tension (Bray, 1995; Heidemann & Buxbaum, 1995; van Essen, 1997) and growth cone advance requires pulling forces supplied either by endogenous growth cone traction forces or exogenous pulling (Lamoureux, Buxbaum & Heidemann, 1989). Moreover, pull exerted on neuronal soma margins lacking neurite outgrowth initiates growth cones in the pulled region (Zheng et al., 1991). Finally, filopodial production is stimulated by shrinking forces (Bray et al., 1991). VLD leading edges in cultured neurons were generated precisely where shrinking forces acted to draw in plasma membrane. We suggest that, like filopodia in growth cones, filopodia in VLDs were stimulated by local mechanical forces. An implication of the 3-D/2-D insert in Fig. 14 is that for neurons, a given mechanical stimulus could, depending on the opportunities provided by the local topology of the adherent substratum, promote either membrane internalization or neurite extension.

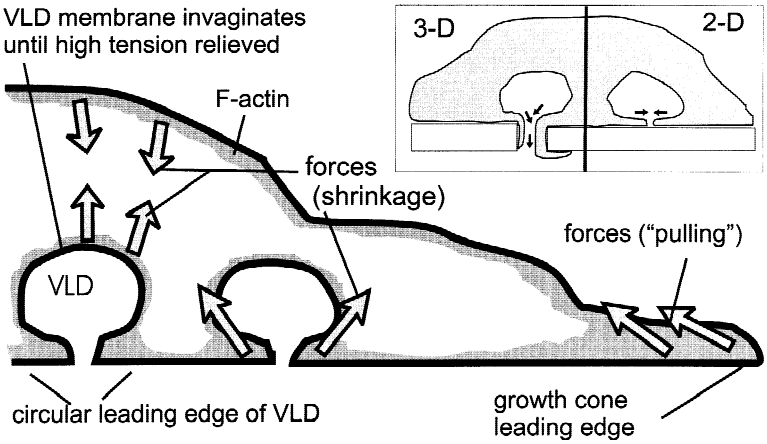

Fig. 14. Cartoon showing similarities between leading edge at VLDs and growth cones. Generalized pulling forces (created by cell shrinkage or other means) are indicated as arrows. We suggest that where a VLD leading edge experiences such forces, F-actin reorganization and/or reassembly is promoted. If a substratum provided crevices ("3-D") instead of being planar ("2-D"), any part of the annular leading edge would presumably have the option of growing "forward" (i.e., downward in the cartoon) not just centripetally. Depending on substratum topology, therefore, mechanosensitive responses of F-actin to applied forces could stimulate either neurite outgrowth or the retrieval of surface membrane.

Parallels with Regulatory Volume Decrease

In the widespread phenomenon of regulatory volume decrease (RVD), shrinkage is cell-mediated and occurs while the medium remains hypotonic. Protrusions that form with swelling are retrieved as RVD proceeds; cytochalasin prevents RVD (e.g., Cornet et al., 1993). While shrinking, cells undergoing RVD (~5 min timeframe) take up bath dye into ~1 μm vacuoles (Czekay et al., 1994), echoing VLD formation and vacuolization in shrinking neurons. In another important parallel, in swollen cells that subsequently undergo RVD, F-actin first disorganizes, then, with shrinkage (~5 min), reorganizes (Cornet et al., 1994). In neurons, VLD recovery is cytochalasin-sensitive (Reuzeau et al., 1995) and we showed that a swell-then-shrink regime first disorganized then reorganized F-actin in the vicinity of invaginating membrane.

We usually elicited VLDs via exogenously driven shrinkage but cell-mediated VLDs were also demonstrated with sustained hyposmia. This hyposmia seemed to elicit a slowly developing RVD plus the small VLDs, raising the possibility of coordinated volume and cell surface area regulation.

In epithelia, swelling-induced increases in intracellular calcium (Ca_{int}) are necessary for RVD, but not in mammalian neurons (Morán et al., 1997). Interestingly, Ca_{int} is irrelevant to all events reported here during 5 min of swelling and 5 min of shrinking in NS; the stimulus used to elicit VLDs (5 min in 50% medium) produces at best a trivial increase (<10%) in Ca_{int} in *Lymnaea* neurons, and after return to NS, Ca_{int} is identical to preswelling levels (Herring et al., 1998). Thus, as with neuronal RVD, calcium signaling is implicated neither during swelling, when F-actin disorganizes, nor subsequently during reshrinking when it reorganizes. In neurons, where calcium signals are used with such finesse in synaptic transmission, it may be preferable to rely on membrane and/or cytoskeleton tension as a primary signal for regulating cell volume and surface area.

Other F-actin Associations with Surface Membrane

F-actin appears at membrane invaginations elsewhere. In growing yeast, where fingerlike invaginations are surrounded by F-actin (Mulholland et al., 1994), wall material evidently deposits within the invagination, enabling yeast to insert new wall material in the face of turgor pressure.

Macrophages have dynamic F-actin-rich membrane invaginations. F-actin organizes at phagocytic cups that engulf objects (Morisaki, Heuser & Sibley, 1995) over 2–4 min (comparable to the reorganization of F-actin at VLDs). Cytoskeletal dynamics at VLDs are also reminiscent of those during the invagination of 1–2 μm macropinocytotic vacuoles in *Dictyostelium* (Hacker, Albrecht & Maniak, 1997), cells in which the actin cytoskeleton is important for withstanding osmomechanical shocks, as seen in the poor survival of cells compromised by knockout of proteins that organize the F-actin network (Rivero et al., 1996).

Leading edge actin at the mouth of VLDs may bear some relation to inductopodia, F-actin bundles which form behind polycationic beads adhering to *Aplysia* growth cones (Forscher, Lin & Thompson, 1992). Cytochalasin reversibly inhibits inductopodial elongation. Inductopodia form immediately upon bead binding and grow to ~5 μm in 1 min. It was proposed that positive charges on the beads sequester or recruit endogenous actin nucleating proteins thereby stimulating F-actin assembly. Both inductopodia and VLD leading edge could be described as rapid adhesion zone-directed F-actin assemblies.

Phalloidin staining in serum-deprived fibroblastic cells resembles substratum staining of lamellae in our control neurons: diffuse filamentous F-actin networks and plentiful puncta (Machesky & Hall, 1997). At high resolution, however, it is evident that some of the puncta (<1 μm) are in fact rings of F-actin. Additionally, the rings are immunopositive for myosin-II and incorporate

new actin monomers with a half-time of ~20 min. Whether these structures participate in membrane retrieval is unknown.

Conclusions

In shrinking adherent neurons, VLDs invaginating from the substratum were foci for a substantial reorganization of F-actin. F-actin provided a continuous coat for the membranous dilation of VLDs and, at the substratum or VLD mouth, it formed dynamic leading edge that could constrict, reinternalizing surface membrane. This suggests that mechanical stresses at the cell surface act jointly on the plasma membrane's bilayer and its cytoskeleton. It seems likely that F-actin dynamics help coordinate surface area and volume regulation. By the same token, the mechanoresponsive cortical cytoskeleton should provide mechanoprotection for the bilayer during morphological change.

This research was supported by grants to CEM and LRM from the Heart and Stroke Foundation of Ontario (T3461) and from NSERC, Canada, and to CSC from National Institutes of Health (NS25789 and DC01785).

References

Andrew, R.D., Lobinowich, M.E., Oshehobo, E.P. 1997. Evidence against volume regulation by cortical brain cells during acute osmotic stress. *Exp. Neurol.* **143:**300–312

Auer, R.N., Coulter, K.C. 1994. The nature and time course of neuronal vacuolation induced by the N-methyl-D-aspartate antagonist MK-801. *Acta Neuropath.* **87:**1–7

Bouchard, M., Pare, C., Dutasta, J.P., Chauvet, J.P., Gicquaud, C., Auger, M. 1998. Interaction between G-actin and various types of liposomes: A 19F, 31P, and 2H nuclear magnetic resonance study. *Biochemistry* **37:**3149–3155

Bray, D., Money, N.P., Harold, F.M., Bamburg, J.R. 1991. Responses of growth cones to changes in osmolality of the surrounding medium. *J. Cell Sci.* **98:**507–515

Bray, D. 1996. Membrane biophysics: the dynamics of growing axons. *Current Biol.* **6:**241–243

Cheng, T.P.O., Reese, T.S. 1987. Recycling of plasmalemma in chick tectal growth cones. *J. Neurosci.* **7:**1752–1759

Cohan, C.S. 1990. Frequency-dependent and cell-specific effects of electrical activity on growth cone movements of cultured *Helisoma* neurons. *J. Neurobiol.* **21:**400–413

Cornet, M., Isobe, Y., Lemanski, L.F. 1994. Effects of anisosmotic conditions on the cytoskeletal architecture of cultured PC12 cells. *J. Morphology* **222:**269–286

Cornet, M., Lambert, I.H., Hoffmann, E.K. 1993. Relation between cytoskeleton, hypo-osmotic treatment and volume regulation in Ehrlich ascites tumor cells. *J. Membrane Biol.* **131:**55–66

Czekay, R., Kinne-Saffran, E., Kinne, R.K.H. 1994. Membrane traffic and sorbitol release during osmo- and volume regulation in isolated rat renal inner medullary collecting duct cells. *Eur. J. Cell. Biol.* **63:**20–31

Dai, J., Sheetz, M.P. 1995. Regulation of endocytosis, exocytosis, and shape by membrane tension. *Cold Spring Harb. Symp. Quant. Biol.* **60:**567–71

Dai, J., Wan, X., Sheetz, M.P., Morris, C.E. 1998. Membrane tension in swelling and shrinking molluscan neurons. *J. Neurosci.* **18:**6681–6692

Dailey, M.E., Bridgman, P.C. 1993. Vacuole dynamics in growth cones: correlated EM and video observations. *J. Neurosci.* **13:**3375–3393

Forscher, P., Lin, C.H., Thompson, C. 1992. Novel form of growth cone motility involving site-directed actin filament assembly. *Nature* **357:**515–518

Forscher, P., Smith, S.J. 1988. Actions of cytochalasins on the organization of actin filaments and microtubules in a neuronal growth cone. *J. Cell. Biol.* **107:**1505–1516

Glogauer, M., Arora, P., Chou, D., Janmey, P.A., Downey, G.P., McCulloch, C.A.G. 1998. The role of actin-binding protein 280 in integrin-dependent mechanoprotection. *J. Biol. Chem.* **273:**1689–1698, 1998

Hacker, U., Albrecht, R., Maniak, M. 1997. Fluid-phase uptake by macropinocytosis in *Dictyostelium. J. Cell Sci.* **110:**105–112

Heidemann, S.R., Buxbaum, R.E. 1994. Mechanical tension as a regulator of axonal development. *Neurotoxicology* **15:**95–108

Henson, J.H., Roesener, C.D., Gaetano, C.J., Mendola, R.J., Forrest, J.N. Jr., Holy, J., Kleinzeller, A. 1997. Confocal microscopic observation of cytoskeletal reorganization in cultured shark rectal gland cells following treatment with hypotonic shock and high external K^+. *J. Exp. Zool.* **279:**415–424

Herring, T.L., Slotin, I.M., Baltz, J.M, Morris, C.E. 1998. Neuronal swelling and surface area regulation: elevated intracellular calcium is not a requirement. *Am. J. Physiol.* **274:**C272–C281

Homann, U. 1998. Fusion and fission of plasma-membrane material accommodates for osmotically induced changes in surface are of guard-cell protoplasts. *Planta* **206:**329–333

Ingber, D.E. 1997. Tensegrity: the architectural basis of cellular mechanotransduction. *Annu. Rev. Physiol.* **59:**575–99

Lamoureux, P., Buxbaum, R.E., Heidemann, S.R. 1989. Direct evidence that growth cones pull. *Nature* **340:**159–162

Lin, C., Lamoureux, P., Buxbaum, R.E., Heidemann, S.R. 1995. Osmotic dilution stimulates axonal outgrowth by making axons more sensitive to tension. *J. Biomechanics* **28:**1429–1438

Lippmann, B.J., Yang, R., Barnett, D.W., Misler, S. 1995. Pharmacology of volume regulation following hypotonicity-induced cell swelling in clonal N1E115 neuroblastoma cells. *Brain Res.* **686:**29–36

Machesky, L.M., Hall, A. 1997. Role of Actin Polymerization and adhesion to extracellular matrix in rac- and rho-induced cytoskeletal reorganization. *J. Cell Biol.* **138:**913–926

Mills, L.R., Morris, C.E. 1998. Neuronal plasma membrane dynamics evoked by osmomechanical perturbations. *J. Membrane Biol.* **166:**223–238

Mills, J.W., Schwiebert, E.M., Stanton, B.A. 1994. Evidence for the role of actin filaments in regulating cell swelling. *J. Exp. Zool.* **268:**111–120

Morán, J., Morales-Mulia, S., Hernandez-Cruz, A., Pasantes-Morales, H. 1997. Regulatory volume decrease and associated osmolyte fluxes in cerebellar granule neurons are calcium independent. *J. Neurosci. Res.* **47:**144–154

Morán, J., Sabanero, M., Meza, I., Pasantes-Morales, H. 1996. Changes of actin cytoskeleton during swelling and regulatory volume decrease in cultured astrocytes. *Am. J. Physiol.* **271:**C1901–C1907

Morisaki, J.H., Heuser, J.E., Sibley, L.D. 1995. Invasion of *Toxoplasma gondii* occurs by active penetration of the host cell. *J. Cell Sci.* **108:**2457–2464

Morris, C.E., Lesiuk, H., Mills, L.R. 1997. How do neurons monitor their mechanical status? *Biol. Bull.* **192:**118–120

Morris, C.E., Williams, B., Sigurdson, W.J. 1989. Osmotically induced volume changes in isolated cells of a pond snail. *Comp. Biochem. Physiol.* **92A:**479–483

Mountain, I., Waelkens, E., Missiaen, L., van Driessche, W. 1998. Changes in actin cytoskeleton during volume regulation in C6 glial cells. *Eur. J. Cell Biol.* **77:**196–204

Mulholland, J., Preuss, D., Moon, A., Wong, A., Drubin, D., Botstein, D. 1994. Ultrastructure of the yeast actin cytoskeleton and its association with the plasma membrane. *J. Cell Biol.* **125:**381–391

Myers, P.Z., Bastiani, M.J. 1993. Growth cone dynamics during the migration of an identified commissural growth cone. *J. Neurosci.* **13:**127–143

Reuzeau, C., Mills, L.R., Harris, J.A., Morris, C.E. 1995. Discrete and reversible vacuole-like dilations induced by osmomechanical perturbation of neurons. *J. Membrane Biol.* **145:**33–47

Rivero, F., Köppel, B., Peracino, B., Bozzaro, S., Siegert, F., Weijer, C.J., Schleicher, M., Albrecht, R., Noegel, A.A. 1996. The role of the cortical cytoskeleton: F-actin crosslinking proteins protect against osmotic stress, ensure cell size, cell shape and motility, and contribute to phagocytosis and development. *J. Cell Sci.* **109:**2679–2691

Sigurdson, W.J., Morris, C.E. 1989. Stretch-sensitive ion channels in growth cones of snail neurons. *J. Neurosci.* **9:**2801–2808

Strange, K. 1993. Maintenance of cell volume in the central nervous system. *Pediatr. Nephrol.* **7:**689–697

Terasaki, M., Chen, L.B., Fujiwara, K. 1986. Microtubules and the endoplasmic reticulum are highly interdependent structures. *J. Cell Biol.* **103:**1557–1568

Terasaki, M., Song, J., Wong, J.R., Weiss, M.J., Chen, L.B. 1984. Localization of endoplasmic reticulum in living and glutaraldehyde-fixed cells with fluorescent dyes. *Cell* **38:**101–108

van Essen, D.C. 1997. A tension-based theory of morphogenesis and compact wiring in the central nervous system. *Nature* **385:**313–318

Wan, X., Harris, J.A., Morris, C.E. 1995. Responses of neurons to extreme osmomechanical stress. *J. Membrane Biol.* **145:**21–31

Welnhofer, E.A., Zhao, L., Cohan, C.S. 1997. Actin dynamics and organization during growth cone morphogenesis in *Helisoma* neurons. *Cell Mot. Cytoskel.* **37:**54–71

Wu, D-Y., Goldberg, D.J. 1993. Regulated tyrosine phosphorylation at the tips of growth cone filopodia. *J. Cell Biol.* **123:**653–664

Zhang, J., Larsen, T.H., Lieberman, M. 1997. F-actin modulates swelling-activated chloride current in cultured chick cardiac myocytes. *Am. J. Physiol.* **273:**C1215–C1224

Zheng, J., Lamoureux, P., Santiago, V., Dennerll, T., Buxbaum, R.E., Heidemann, S.R. 1991. Tensile regulation of axonal elongation and initiation. *J. Neurosci.* **11:**1117–1125

Ziv, N.E., Spira, M.E. 1998. Induction of growth cone formation by transient and localized increases of intracellular protolytic activity. *J. Cell Biol.* **140:**223–232

Ziyadeh, F.N., Mills, J.W., Kleinzeller, A. 1992. Hypotonicity and cell volume regulation in shark rectal gland: role of organic osmolytes and F-actin. *Am. J. Physiol.* **262:**F468–F479